LENS INCLINATION DUE TO INSTABLE FIXINGS DETECTED AND VERIFIED WITH VDI/VDE 2634 PART 1

C. Haig [a] *, C. Heipke [b], M. Wiggenhagen [b]

[a] VOLKSWAGEN AG, Berliner Ring, Letter box 1785, 38436 Wolfsburg, Germany – claudia.haig@volkswagen.de
[b] Institute of Photogrammetry and GeoInformation, Leibniz Universität Hannover, Nienburger Str. 1, 30167 Hanover, Germany

Commission V, Working Group V/1

KEY WORDS: Close Range, Metrology, Calibration, Adjustment, Modelling, VDI/VDE guideline 2634 Part 1

ABSTRACT:

The automotive industry increasingly uses close range photogrammetry systems with bundle adjustment for acquiring 3D information to check for example the quality of sheet metal parts. Because of its flexibility, at times a photogrammetric system is used in climate chambers and hence is exposed to extreme strain. The interior orientation of the camera whilst capturing in the difficult environment can not be assumed to be stable and an appearance of wear may occur over time. This paper presents the effect of unstable lens fixings. A practical adaptation for reducing the lens movement, whereby the commonly used ring flash is dissociated from the lens, is introduced and successfully tested. Also, a mathematical model to compensate the effect of lens inclination is presented and verified by the German guideline VDI/VDE 2634 Part 1. First results show significant improvement in maximum length variation, which is the desired parameter in the guideline VDI/VDE 2634 part 1.

1. INTRODUCTION

1.1 Background

The demand for high precision measuring techniques in industrial environments has continuously increased in the last 10 - 15 years. Camera based techniques have competed against other high precision measuring instruments such as CMMs (Coordinate Measuring Machines), laser trackers and GPS-like techniques (Indoor GPS). Close range photogrammetry with cameras has various advantages over most of the listed systems. It is very flexible in handling, does not need a fixed space such as the CMM, data is captured very fast – machines in production lines do not have to stop for long periods of time – coordinates are captured in a non-contact manner and with additional image analysis methods, feature lines or sections on for example metal sheets can be measured. One example of photogrammetry in an extreme application is a measurement in a climate chamber. With temperature variations from -40°C up to 90°C, pressure of time, constriction in space and the amount of obtainable points, apart from camera based photogrammetry non of the listed techniques can still operate. The cameras are under great stress while operating in very hot or cold environments and among other effects the interior orientations can not necessarily be assumed to remain stable.

In industry a photogrammetric system is also increasingly used as reference for other measuring tools such as for example fringe projection. However, as these tools have improved over time, results from photogrammetry with bundle adjustment and consumer cameras can not necessarily be expected to be sufficiently accurate any longer. Nevertheless, specific metric cameras may be too expensive.

Cameras utilised at VOLKSWAGEN are consumer cameras and not specific stable metric cameras. It is assumed that the lens mount is not firmly fixed to the camera body. Therefore, the lens follows gravity and in general the optical axis is not perpendicular to the image plane any longer. As a consequence image coordinates are distorted. To compensate for this effect a "virtual" chip movement needs to be introduced into the model of the interior orientation (see also Hastedt et al., 2002).

The remainder of this paper is organised as follows: section 2 provides a more detailed view about the requirements of camera based techniques in automotive industry as laid down in the German guideline VDI/VDE 2634 part 1 and some related work. Section 3 describes and analyses a new practical solution of enhancing accuracies with an adapter solution for ring flash applications. The mathematical model for rectifying the camera orientation depending on lens inclination is described and tested in section 4. Conclusions and future work can be found in section 5.

2. RELATED WORK

2.1 VDI/VDE guideline 2634 Part 1

Like every other measuring device, photogrammetric systems (in close range photogrammetry commonly summarised as one camera and its allocated scale bars) need to be monitored based on existing accuracy specifications. For this purpose VDI/VDE (Association of German Engineers / Association for Electrical, Electronic & Information Technologies) developed the guideline 2634 part 1 which established the opportunity to compare different photogrammetric systems by the same parameters. Using the length deviation as a criterion VDI/VDE describes one way of monitoring the systems but in fact also enables a comparison with other measuring tools (CMM, laser tracker, etc.). To calculate the maximum length deviation (maximum difference between calibrated and computed length of all scale bars) only one scale bar is introduced into the bundle adjustment as length definition.

Depending on normal workday applications the measuring volume of the calibrating frame needs to be defined. At VOLKSWAGEN a frame with dimensions of approximately 1.5 x 2 x 2 m³ is used (Figure 1 left). According to the guideline a minimum of seven scale bars have to be fixed to the frame to

---

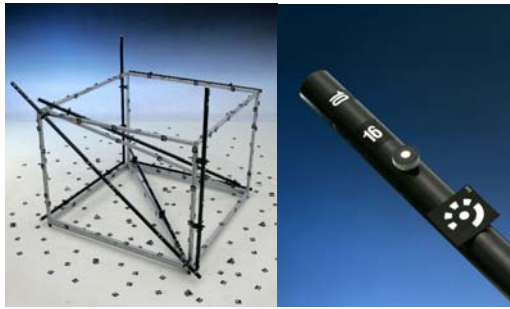cover each corner of the volume with at least one measuring point of a scale bar.

Figure 1: Left – VDI/VDE frame with eight scale bars, Right – scale bar with epoxy resin target and coded target

VOLKSWAGEN applies eight scale bars which are calibrated with a measurement uncertainty of 5 µm over a length of up to 2.6 m. White targets made of epoxy resin (Figure 1 right) are used in the scale bars because of their good attributes such as circularity and a precisely defined edge at the transition from black to white. Retro reflective, contrary to epoxy resin targets are necessary for some special applications but give unsatisfactory results for high accuracy approaches due to shifting effects caused by the characteristics of the retro reflective material (Dold, 1997; Otepka, 2004).
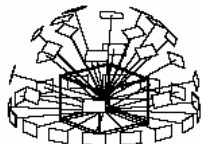

Figure 2: Example for a circular camera set up (Rautenberg, Wiggenhagen, 2002)

The targets fixed to the frame, the targets on the scale bars and the targets inside the measuring volume are captured circulating the frame in four different height planes (Figure 2) with an average of around 120 images.

By using one reference scale bar the calibrated measurement uncertainty (here 5 µm for 2.6 m) needs to be at least one-fifth of the detectable measurement uncertainty (VDI/VDE, 2002, Chapter "Artefacts"). For an accuracy demand of 1:100,000 with these scale bars the measurement uncertainty, which must be obtained, is 26 µm, hence the detectable measurement uncertainty of 25 µm is satisfactory.

2.2 State of the art

The prospect of achieving relative accuracies of 1:100,000 verified with the guideline 2634 part 1 (VDI/VDE, 2002) established by VDI/VDE has been discussed and analysed by various authors (Hastedt et al., 2002; Hastedt, 2004; Luhmann, 2004; Rautenberg, Wiggenhagen, 2002; Rieke-Zapp et al., 2005). The largest accuracy achievement is assumed to be the improvement of the model of the interior orientation.

In principle all advanced interior orientation models for camera based techniques are based on Brown's parameters (Brown, 1971). Hastedt et al. (2002) implemented an image-variant interior orientation using the finite elements method to model the surface of the CCD sensor. The results showed gravity influences as well as heating effects due to the storage unit. Also a shift of the CCD sensor could be assessed and corrected. Furthermore, Hastedt (2004) presented a Monte-Carlo-simulation to modify specific parameters such as systematic effects to model the influence for analysing purposes. Fryer

(1989) and Fraser, Shortis (1992) describe attempts which take distant dependent parameters into account. Rautenberg, Wiggenhagen (2002) tested different camera configurations for the VDI/VDE guideline 2634 part 1 (see Figure 2).

3. A PRACTICAL ADAPTER SOLUTION FOR REDUCING MAXIMUM LENGTH DEVIATIONS

3.1 General

Higher accuracy applications require simultaneous camera calibrations within the bundle adjustment process. Most of the software solutions only work with the common ten Brown parameters for the interior orientation (focal length, principal point in x and y, three parameters for the radial-symmetric distortion, two parameters for the radial-asymmetric and tangential distortion and two parameters for affinity and shear). Mechanical instabilities are mostly not directly considered. Two main mechanical problems can be identified. Whereas the camera body and the lens itself can be assumed to be stable, chip fixations can be instable as has been discussed for example by Hastedt et al. (2002). Another crucial area is the lens fixing to the camera body. In close range photogrammetry, where consumer cameras dominate, the fixing is usually a bayonet. If due to a frequently lens changing or other circumstances the bayonet fixing does not hold the lens tightly to the camera body a tilt of the lens may occur.

3.2 Adapter solution

Camera based systems in close range applications are mostly used with a ring flash mounted on the filter thread at the end of the lens. Figure 3 shows an example of such a photogrammetric system.

Figure 3: Tritop System of Company GOM (© GOM, Braunschweig)

Due to the presumption that the lens might not be firmly fixed to the camera body, a ring flash mounted at the end of the lens will cause effects of leverage.

In approximation the lens can be assumed to be rigid, of constant density and tilts in one point. This point is assumed to be the centre of the bayonet. By adding extra weight at the end of the lens the tilting angle increases. Equation 1 shows an abstracted calculation and figure 4 shows this effect schematically.
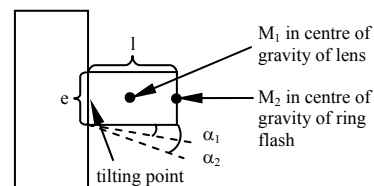

Figure 4: Schematic description of the calculation of the influence of the extra weight of the ring flash

$$\frac{\alpha_1}{K_1} = \frac{\alpha_2}{K_1 + K_2}$$

$$K_1 = \frac{M_1 \cdot \dfrac{l}{2}}{\dfrac{e}{2}} ; K_2 = \frac{M_2 \cdot l}{\dfrac{e}{2}}$$

(1)

where: $\alpha_{1,2}$ =   tilting angle (1 without ring flash, 2 with ring flash)
       M_1 =   lens weight
       M_2 =   ring flash weight
       l =   lens length
       e =   lens diameter

For M_1 = 265 g, M_2 = 140 g, l = 4.65 cm, e = 3.1 cm (measures of a Nikkor 24 mm lens) α_2 equals $2.05 \cdot \alpha_1$. This effect therefore should not be underestimated since it leads to distortions and the interior orientation can no longer expected to be stable throughout a set of measurements.

To investigate possible lens movement, an adapter (Figure 5) to separate the lens and the ring flash has been built and tested.
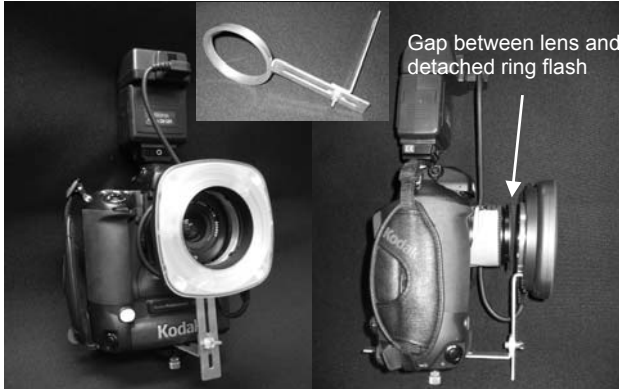

Figure 5: Middle – Adapter for ring flash,
left and right – ring flash mounted on the adapter

Two cameras and configurations with and without the adapter were tested according to the VDI/VDE guideline 2634 part 1.

1.   Ring flash mounted on the lens
2.   Ring flash mounted on the adapter

The cameras used were a Kodak DCS 660 and a Fuji S2 Pro both with wide angle lenses (24 mm). The image acquisition was carried as described in section 2.1. Photogrammetric processing included a bundle adjustment with self calibration using the ten Brown parameters. Maximum length deviations were calculated in comparison to the reference scale bar.

An improvement of maximum length variations of 20 – 30 µm between configuration 1 and 2 was obtained, which represent an accuracy enhancement of 25-28 %, see figure 6. Both cameras show significant differences between the two configurations but keep the characteristic that the Fuji S2 Pro is marginally better than the Kodak DCS 660.

In this study relative accuracies of up to 1:33,590 (equivalent to a maximum length deviation of 0.0774 mm divided by the scale bar length of 2.6 m) could be achieved.

To detach the ring flash from the lens with an adapter is a practical solution to decrease errors probably caused by an unstable lens fixing. The lens itself however still causes errors due to a tilt of the optical axis depending on the orientation of the camera with respect to gravity.
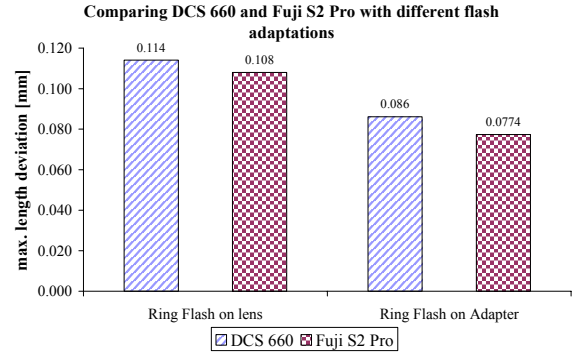

Figure 6: Diagram to show results of different flash configurations

4. MATHEMATICAL MODEL FOR COMPENSATING LENS INCLINATION

4.1 Theory and assumptions

Compensation of lens instabilities can be modelled with a tilt of the CCD-chip with respect to the optical axis, resulting in one additional parameter – the lens tilting angle α in the bundle adjustment. During the image capturing the camera is usually orientated in different directions. Therefore, the principal point and the focal length may vary per image. With the changes of the principal point the radial and tangential distortions also may shift marginally.
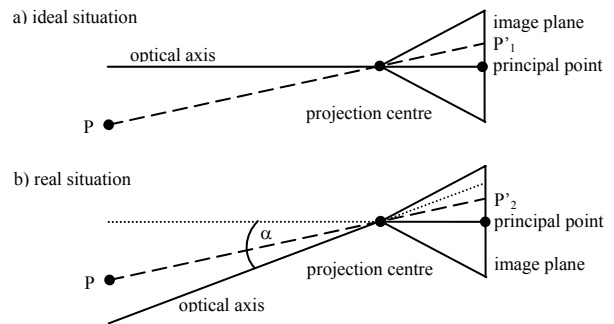

Figure 7: relations between optical axis and image plane

For simplicity it is assumed that the tilting point concurs with the perspective centre* and the lens follows gravity (Figure 7). A maximum tilting angle α_{max} is defined and occurs when the optical axis is horizontal. The individual tilting angle α for a non-horizontal direction of the optical axis is computed by calculating the angle ν between the direction of the gravity vector $\vec{g}$ and the vector in the direction of the optical axis (see section 4.2). This angle is ninety degrees when the tilting angle is a maximum.

4.2 Mathematical Model

The mathematical model is separated in two steps, whereby calculations in step one are carried out in a global coordinate system and step two is computed in an extended image coordinate system.

Step 1
As mentioned before the tilting angle α depends on the direction of the optical axis of the camera. In order to describe

this dependence the angle ν between the gravity vector $\vec{g}$ and the optical axis needs to be determined. ν can be obtained from the angles of exterior orientation. The element r_{33} of the rotation matrix is equivalent to $\cos \nu$ (see Schwidefsky, Ackermann, 1976). Given a sequence of rotations of $\omega \varphi \kappa$ (primary, secondary, tertiary rotation) r_{33} can be described as shown in equation 2. α is then adapted for each image as followed (see also figure 8).
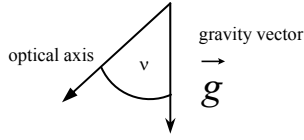

Figure 8: Calculation of angle ν

$$r_{33} = \cos\omega \cdot \cos\kappa$$
$$\upsilon = \arccos(r_{33}) \qquad (2)$$
$$\alpha = \alpha_{max} \cdot \sin\upsilon$$

where: ω = exterior orientation angle
$\quad\quad\;\; \varphi$ = exterior orientation angle
$\quad\quad\;\; r_{33}$ = element of the rotation matrix
$\quad\quad\;\; \alpha_{max}$ = maximum tilting angle

Step 2

In the second step the model is conceived in the image coordinate system. The image plane E_1 and the optical axis in figure 9 represent the ideal configuration of the relation between image plane and optical axis, whereby the image plane is perpendicular to the optical axis. If a lens follows gravity because of a loose bayonet fixing and this new optical axis is aligned with the original optical axis on the object side the related image plane E_2 is tilted with respect to E_1. In figure 9 this situation is shown for a horizontal optical axis, where as mentioned before the tilting angle is a maximum.
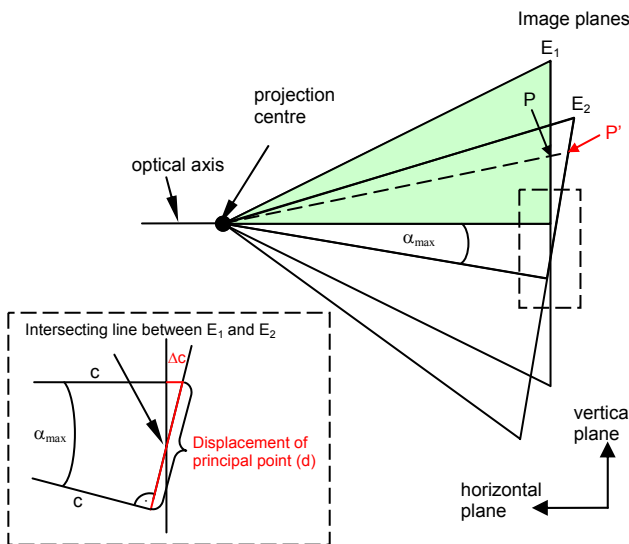

Figure 9: 2D-case for principal point displacement and focal length variation

E_1 corresponds to the image plane depicted in figure 7a an E_2 to that shown in figure 7b after the optical axis has been aligned with the horizontal direction. Thus, object point P lies at position P' on E_2. As the use of a standard bundle adjustment

process is desired, firstly the image coordinates of P with respect to image plane E_1 have to be computed.

Given that the light beam from the perspective centre does not expose the CCD-chip with parallel rays of light, the tilting of the image plane needs to be modelled in three dimensions. For this approach a coordinate system XYZ centred in the perspective centre is introduced (see figure 10). The axis Z points parallel to the ideal optical axis. Axis X is parallel to horizon and also parallel to the image coordinate axis x of the ideal configuration (E_1) if the camera is orientated horizontally as in figure 10. Y is chosen to obtain a right-handed system.
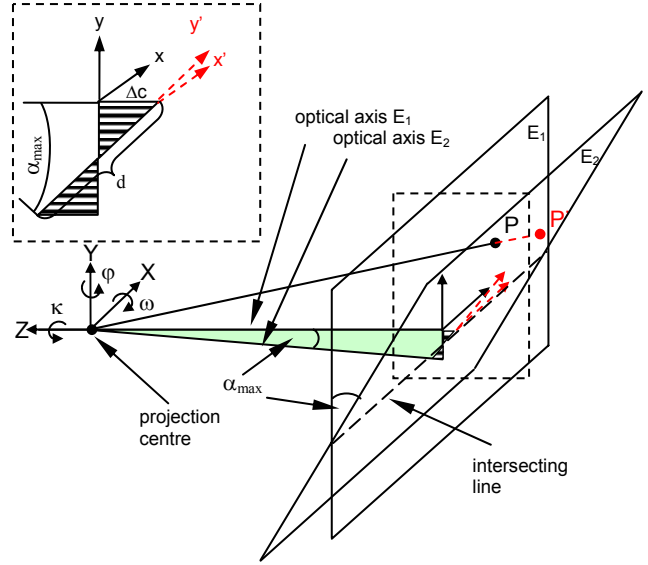

Figure 10: Model for lens tilting with E_1 ideal chip plane and E_2 inclined real chip plane at a horizontal orientation where α is maximum

Regardless of the exterior orientation parameters, only the image points at the intersecting line of the two planes E_1 and E_2 are not distorted; the respective coordinates are merely shifted by the displacement of the principal point (see figure 10):

$$d = \tan\alpha \cdot c$$
$$\Delta x_{PP}' = -\sin\kappa \cdot d \qquad (3)$$
$$\Delta y_{PP}' = \cos\kappa \cdot d$$

where: d = principal point displacement
$\quad\quad\;\; c$ = focal length
$\quad\quad\;\; \alpha$ = inclination angle of the image
$\quad\quad\;\; \Delta x_{PP}$ = principal point shift in x
$\quad\quad\;\; \Delta y_{PP}$ = principal point shift in y
$\quad\quad\;\; \vec{x}'$ = image coordinate vector in E_2
$\quad\quad\;\; \kappa$ = angle between horizontal plane (X-Z-plane) and x'-axis of the image coordinates

The focal length distortion is also image dependent because α changes from one image to the next, see equation 4 and figure 9.

$$c' = \frac{c}{\cos\alpha} \qquad (4)$$
$$\Delta c = c' - c$$

where: c = focal length
α = inclination angle of the image
Δc = elongation of focal length
c' = new focal length for image plane E_2

Next, the planes E_1 and E_2 are set up in terms of equations, followed by the computation of corrected image coordinates of point P on E_1. For plane E_1 the pointing vector is collinear to the optical axis and contains only the value of the focal length. One direction vector $\vec{b}_1$ is perpendicular to gravity and the other direction vector $\vec{c}_1$ points opposite gravity.

Plane E_2 is defined with the pointing vector parallel to the pointing vector of E_1 but with the length of c'. The direction vector $\vec{b}_2$ is identical to $\vec{b}_1$. Vector $\vec{c}_2$ is defined taking the inclination angle α into account. $\vec{c}_{2n}$ is the related normalised vector of unit length.

$$\text{Parameterform}: \vec{x}_1 = \vec{a}_1 + r_1 \cdot \vec{b}_1 + s_1 \cdot \vec{c}_1$$
$$E_1: \quad \vec{x}_1 = \begin{pmatrix} 0 \\ 0 \\ -c \end{pmatrix} + r_1 \begin{pmatrix} \cos\kappa \\ -\sin\kappa \\ 0 \end{pmatrix} + s_1 \begin{pmatrix} \sin\kappa \\ \cos\kappa \\ 0 \end{pmatrix} \quad (5)$$

$$\text{Parameterform}: \vec{x}_2 = \vec{a}_2 + r_2 \cdot \vec{b}_2 + s_2 \cdot \vec{c}_2$$
$$E_2: \vec{x}_2 = \begin{pmatrix} 0 \\ 0 \\ -c' \end{pmatrix} + r_2 \begin{pmatrix} \cos\kappa \\ -\sin\kappa \\ 0 \end{pmatrix} + s_2 \begin{pmatrix} \sin\kappa \\ \cos\kappa \\ -\tan\alpha \end{pmatrix}; \quad (6)$$
$$s_2 \begin{pmatrix} \sin\kappa \\ \cos\kappa \\ -\tan\alpha \end{pmatrix} = s_{2n} \begin{pmatrix} c_{2x} / \left(\sqrt{c_{2x}^2 + c_{2y}^2 + c_{2z}^2}\right) \\ c_{2y} / \left(\sqrt{c_{2x}^2 + c_{2y}^2 + c_{2z}^2}\right) \\ c_{2z} / \left(\sqrt{c_{2x}^2 + c_{2y}^2 + c_{2z}^2}\right) \end{pmatrix}$$

Next, we describe the straight line running through the projection centre and the uncorrected point P' on E_2 (see figure 10). This straight line can be calculated whereby the pointing vector $\vec{a}_3$ equals zero, (0, 0, 0), and the direction vector $\vec{b}_3$ runs from the perspective centre to the image point P' on E_2 corrected by the shift of the principal point (Equation 7).

$$g: \vec{x}_3 = \vec{a}_3 + v \cdot \vec{b}_3$$
$$= \begin{pmatrix} 0 \\ 0 \\ 0 \end{pmatrix} + v \begin{pmatrix} b_{2x} \cdot (x_{P'} - \Delta x_{PP}') + c_{2nx} \cdot (y_{P'} - \Delta y_{PP}') \\ b_{2y} \cdot (x_{P'} - \Delta x_{PP}') + c_{2ny} \cdot (y_{P'} - \Delta y_{PP}') \\ -c - b_{2y} \cdot c_{2nz} \cdot b_{3x} - (-b_{2x} \cdot c_{2ny} \cdot b_{3y}) \end{pmatrix} \quad (7)$$

where: $x_{P'}$ and $y_{P'}$ are uncorrected image point coordinates
b_{3z} is derived by calculating the z coordinate of E_2 by using $x_{P'}$ and $y_{P'}$ with the correction of the principal point displacement

The straight line g intersects image plane E_1 in P. This intersecting point is the corrected image point. It's coordinates can be calculated with equation 8.

$$\begin{pmatrix} X_i \\ Y_i \\ Z_i \end{pmatrix} = v \begin{pmatrix} b_{2x} \cdot (x_{P'} - \Delta x_{PP}') + c_{2nx} \cdot (y_{P'} - \Delta y_{PP}') \\ b_{2y} \cdot (x_{P'} - \Delta x_{PPP}') + c_{2ny} \cdot (y_{P'} - \Delta y_{PP}') \\ -c - b_{2y} \cdot c_{2nz} \cdot b_{3x} - (-b_{2x} \cdot c_{2ny} \cdot b_{3y}) \end{pmatrix} \quad (8)$$

where: X_i, Y_i, Z_i = intersecting point on E_1 and $Z_i \equiv -c$

Finally, the corrected image point P needs to be transformed into the original image coordinate system (Equation 9).

$$x_P = \cos(-\kappa) \cdot X_i + \sin(-\kappa) \cdot Y_i \quad (9)$$
$$y_P = -\sin(-\kappa) \cdot X_i + \cos(-\kappa) \cdot Y_i$$

In equation 9 x_P and y_P are the image coordinates corrected for the effect of lens inclination.

With a configuration of lens tilting in the projection centre a camera with 24 mm focal length an angle α_{max} of 0.05° would cause a principal point shift of 3.9 pixel at a pixel size of 5.42 μm. Table 1 presents distortion parameters for different configurations, computed with a pixel size of 5.42 μm, a focal length of 24 mm (equivalent to 4428 pixels) and principal point coordinates of x_{PP} = 2.5 pixels and y_{PP} = 7.1 pixels.

Camera Orientation horizontal (κ = 0°)

Tilting angle α_{max} in [deg]	0.01°	0.1°	0.5°
c distortion in [pix]	0.0001	0.0067	0.1686
PP distortion in x in [pix]	0	0	0
PP distortion in y in [pix]	0.8	7.7	38.6

Camera Orientation inclined (κ = 45°)

Tilting angle α_{max} in [deg]	0.01°	0.1°	0.5°
c distortion in [pix]	0.0001	0.0067	0.1686
PP distortion in x in [pix]	-0.546	-5.465	-27.325
PP distortion in y in [pix]	0.546	5.465	27.325

Table 1: Distortions for focal length and principal point

The numerical values demonstrate that the investigated effect does in fact have rather large consequences, although a tilting angle of 0.5° is unlikely to occur due to lens fixings. More likely are angles of approximately 0.01° which still distort the principal point by nearly 1 pixel. It should also be noted that the distortions in the corners of the image plane are obviously larger. Thus, it seems to be beneficial to integrate the tilting effect into the bundle adjustment, if a loose bayonet needs to be taken into account.

4.3 Evaluation

The described model for correcting the effect of lens movement has been applied to three different projects. All projects have been carried out in accordance with the German guideline VDI/VDE 2634 part 1 and have been computed with bundle adjustment and simultaneous camera calibration using the ten Brown parameters. The used camera (Fuji S2 Pro) was equipped with a flash mounted on top of the camera body to eliminate possible interferences from the ring flash. 200 images were taken in project 1, equally rotated around the optical axis, whereas projects 2 and 3 had about 100 – 120 images each. In project 3 most images were acquired with a κ-rotation close to zero. The correction for the image points has been calculated offline and after that the bundle adjustment with the ten Brown parameters has been computed again.
The different projects all show an enhancement in their maximum length deviation (Figure 11). In project 1 the length deviation is reduced by 45 %, in project 2 by 23 % and in project 3 by 7 %. Relative accuracies of up to 1:55,200 were achieved.

Comparing length deviations before and after the corrections of the mathematical model
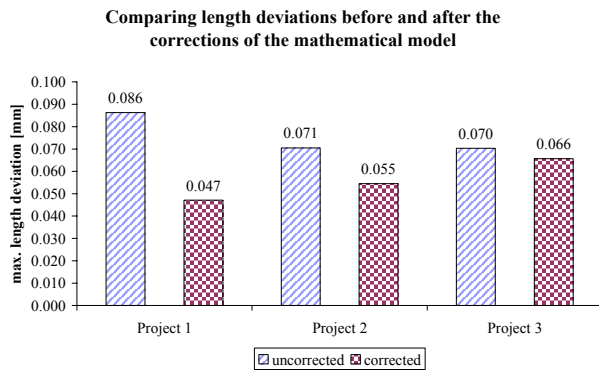

Figure 11: Maximum length deviation for uncorrected and corrected lens inclination

The best result was achieved in project 1. The effect of the lens tilting has a bigger effect in project 1 in which the images were rotated around the optical axis more than in the other projects. This is also indicated by the higher length deviation before corrections were computed. Project 3 shows only little enhancements. Most of the images were taken horizontally and only a few images were rotated. It is assumed that because of this reason most of the tilting effect was compensated by changes in the exterior and interior orientation.

All calculations and image point corrections were computed offline because at the moment the unknown tilting angle is not yet introduced into the bundle adjustment process. The determination of the maximum tilting angle, as in the bundle adjustment, was therefore derived by manual iteration. Figure 12 shows the different results for Project 2.

Different angles for computing max. lenght deviations
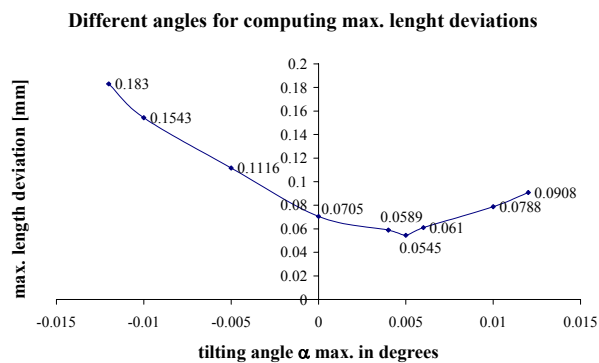

Figure 12: maximum length deviations for different maximum tilting angles

The parabolic graph indicates that this new parameter has a high potential to improve the maximum length deviation.

5. CONCLUSIONS AND FUTURE WORK

The presented paper describes the effect of lens movement. A practical approach to reduce the resulting errors with an adapter solution has been successfully implemented. All investigations are verified by the VDI/VDE guideline 2634 part 1. Improvements of 25-28 % were monitored and evaluated.

Also a model for compensating lens movement due to gravity and unstable fixings has been introduced and tested. This has been modelled with a "virtual" chip movement. First results show improvements of up to 45 % which corresponds to 1:55,200 relative accuracy and allows the automotive industry to securely achieve accuracies under 1/10 mm for a car size measurement volume.

In future work the tilting angle α_{max} will be introduced as an additional unknown parameter into the bundle adjustment process, and further tests will be carried out. Also, possible correlations between the common unknowns and the new parameter for lens movement have to be evaluated and analysed, and a comparison to models of interior orientation used in other disciplines will be made.

REFERENCES

Brown, D.C., 1971. Close-Range Camera Calibration. *Photogrammetric Engineering*, 37(8), pp. 855-866.

Dold, J., 1997. Ein hybrides photogrammetrisches Industrie-Meßsystem höchster Genauigkeit und seine Überprüfung. *Schriftenreihe Universität der Bundeswehr München*, Heft 54.

Fraser, C.S., Shortis, M.R., 1992. Variation of distortion within the photographic field. *Photogrammetric Engineering and Remote Sensing,* 58(6), pp 851-855.

Fryer, J., 1989. Camera Calibration in Non Topographic Photogrammetry. *Handbook of Non Topographic Photogrammetry, American Society of Photogrammetry and Remote Sensing,* 2. run, pp. 51-69.

Hastedt, H., Luhmann, T., Tecklenburg, W., 2002. Image-variant interior orientation and sensor modelling of high-quality digital cameras. *ISPRS Symposium Commission V, Corfu, Greece, The International Archives of the Photogrammetry, Remote Sensing and Spatial Information Science*, 34(5).

Hastedt, H., 2004. Monte-Carlo-Simulation in close-range Photogrammetry. *ISPRS Symposium Commission V, Istanbul, Turkey, The International Archives of the Photogrammetry, Remote Sensing and Spatial Information Science,* 35(5), pp. 18-23.

Luhmann, T. 2004. Messgenauigkeit und Kameramodellierung – Kernfragen der Industriephotogrammetrie. *Photogrammetrie, Fernerkundung, Geoinformation (PFG)*, 2004(1), pp. 13-21.

Maas, H-G., 1999. Ein Ansatz zur Selbstkalibrierung von Kameras mit instabiler innerer Orientierung. *Publikationen der DGPF*, 7, pp. 47-53

Otepka, J., 2004. Precision Target Mensuration in Vision Metrology. Dissertation IPF, TU Wien, http://www.ipf.tuwien.ac.at/phdtheses/diss_jo_04.pdf (accessed: 10.07.2006).

Rautenberg, U., Wiggenhagen, M., 2002. Abnahme und Überwachung photogrammetrischer Messsysteme nach VDI 2634, Blatt 1. *Photogrammetrie, Fernerkundung, Geoinformation (PFG)*, 2002(2), pp. 117-124.

Rieke-Zapp, D., Oldani, A., Peipe, J., 2005. Eine neue hochauflösende Mittelformatkamera für die digitale Nahbereichsphotogrammetrie. *Publikationen der DGPF,* 14, pp. 263-270.

Schwiedefsky, K., Ackermann, F., 1976. Photogrammetrie Grundlagen, Verfahren, Anwendungen. B.G. Teubner Stuttgart, 7th run, pp 27

VDI/VDE, 2002. Guideline 2634 part 1, Optical 3D measuring systems - Imaging systems with point-by-point probing. *VDI/VDE-Gesellschaft Mess- und Automatisierungstechnik.*